

**Identification of Ypk1 as a Novel Selective Substrate for Nitrogen  
Starvation-triggered Proteolysis Requiring Autophagy System and ESCRT  
Machinery**

**Mitsugu Shimobayashi, Hiromu Takematsu, Kazuo Eiho, Yukari Yamane,  
Yasunori Kozutsumi**

**SUPPLEMENTAL TEXT**

**Effect of *SSA1* or *SSA2* deletion on nitrogen starvation-induced Ape1 maturation and Ypk1 proteolysis.**

HSP70-mediated vacuolar delivery was originally reported in an *in vitro* study using isolated nitrogen-starved vacuoles to demonstrate that cytosolic proteins could be incorporated into the vacuole fraction (S1). Subsequently, two groups reported that Hsp70 proteins incorporate Ape1 into vacuoles (S2, S3). However, considerable discrepancies exist between these two reports, in terms of both the Hsp70 isoforms involved in this pathway and nitrogen starvation specificity. Silles *et al.* reported that Ssa1 (Hsp70 isoform) is responsible for Ape1 maturation, in both nutrient-rich and nitrogen-starved conditions (S2). On the other hand, Satyanarayana *et al.* reported that both Ssa1 and Ssa2 are involved in this pathway in nutrient-rich conditions and that the inhibition of Ape1 maturation in *ssa2* $\Delta$  cells is suppressed by autophagy in nitrogen-starved conditions (S3). Thus, we first examined the isoform of Hsp70 to determine whether the deletion of *SSA1* or *SSA2* in a yeast strain (BY4741) leads to a deficiency in this pathway. In contrast to the above two studies, we did not find any differences in Ape1 maturation, as determined by Western blot analysis, for either *ssa1* $\Delta$  or *ssa2* $\Delta$  cells in nitrogen-containing SD culture conditions (Fig. S3B-C). A prominent decrease in mApe1 accumulation was observed only in *ssa1* $\Delta$  cells when nitrogen was omitted from medium (Fig. S3B-C). Silles *et al.* studied Ape1 maturation using a [<sup>35</sup>S]-methionine/cysteine pulse-chase assay with the temperature-sensitive allele of *SSA1* and deletions of *SSA2*, *SSA3*, and *SSA4*, which correspond to other members of the cytosolic Ssa subfamily; therefore, their result may not be replicable with our prApe1 detection on Western blots of single *ssa1* $\Delta$  cells. Nonetheless, the results in Fig. S3B-C tend to support the idea that Ssa1 is responsible for Ape1 maturation in nitrogen-starved conditions. Despite the delay in Ape1 maturation, Ypk1

stability was not affected in nitrogen-starved *ssa1* $\Delta$  cells, indicating that Ssa1 is not required for nitrogen starvation-induced Ypk1 proteolysis. This implies that HSP70-mediated vacuolar delivery is not involved in the vacuolar sorting of Ypk1 upon nitrogen starvation.

## SUPPLEMENTAL MATERIALS AND METHODS

*Semi-quantitative RT-PCR (sqRT-PCR)* —Total RNA was prepared using the hot phenol method and digested with DNase I (Ambion). Random hexamer-primed cDNA was prepared by a reverse transcriptase (MMLV-RT, invitrogen) in the presence of a RNase inhibitor (SUPERase-In, Ambion) at 42 °C for 1 h. Pairs of gene-specific PCR primers and the number of cycles used for each of the transcripts are listed in Table S1. PCR was performed in the quantifiable range using a serial dilution of the total RNA.

Table S1. List of primers and cycle numbers for sqRT-PCR

mRNA	Primer sequence	Amplicon size (bp)	Cycles
<i>YPK1</i>	5'-TATTCTTGGAAGTCAAAGTTTAAGT-3'	529	27
	5'-TTGGTTCTTTATTTGAACACGGGAC-3'		
<i>ACT1</i>	5'-AGGTTGCTGCTTTGGTTATTGATAA-3'	298	25
	5'-AACAGGGTGTCTTCTGGGGCAACT-3'		

## SUPPLEMENTAL MOVIE LEGEND

**SUPPLEMENTAL MOVIE 1. GFP-Ypk1 is sorted into vacuoles upon nitrogen starvation.**

3D image of FM4-64 (*red*)-stained *pep4* $\Delta$  expressing GFP-Ypk1 (*green*). Images in Z-sections were acquired at 0.2  $\mu$ m intervals by a laser-scanning confocal microscope and reconstructed into a 3D movie. A selected image of the Z-stacks is shown in Fig. 2E.

## SUPPLEMENTAL FIGURE LEGENDS

**FIGURE S1. *YPK1* mRNA expression is not reduced upon nitrogen starvation.**

Time-course analysis of *YPK1* mRNA expression in WT cells upon nitrogen starvation (NS). Expressions of *YPK1* and *ACT1* (a loading control) were determined by semi-quantitative reverse transcription polymerase chain reaction (sqRT-PCR). The control shows that the RT-PCR reactions were in the quantifiable range.

**FIGURE S2. N-terminal GFP-fused Ypk1 localizes in cytoplasm in WT cells.**

Fluorescence microscopic analysis of GFP-Ypk1 in logarithmically growing WT cells harboring pRS415-*GFP-YPK1*. Bar, 5  $\mu$ m.

**FIGURE S3. Cvt pathway and HSP70-mediated vacuolar delivery are not involved in nitrogen starvation-induced Ypk1 proteolysis.**

(A-B) Time-course analysis of Ypk1 expression in nitrogen-starved WT, *atg11* $\Delta$  (A), *ssa1* $\Delta$  (B), and *ssa2* $\Delta$  (B) cells. Logarithmically growing cells were starved of nitrogen (NS) for the times indicated. Total cell lysates were prepared at the indicated time points. The proteins were resolved by SDS-PAGE and analyzed on Western blots using antibodies against Ypk1 (two bands), Ape1, and Pgc1, a loading control. The processing of premature Ape1 (prApe1) to mature Ape1 (mApe1) is shown as a positive control for the *ATG11*, *SSA1*, or *SSA2* deletions. (C) Relative processing of Ape1 (compared with 3 h-WT) in WT, *ssa1* $\Delta$ , or *ssa2* $\Delta$  cells. mApe1 and Ypk1 signal intensities were normalized to that of Pgc1 and plotted on a line graph as the means of four independent experiments. Error bars indicate SEMs. An asterisk show statistical significance at  $P < 0.05$ , determined using

Student's *t*-test.

**FIGURE S4. Involvement of ESCRT machinery in autophagy-related vacuolar sorting of GFP-Ypk1**

Fluorescence microscopic analyses of GFP-Ypk1 localization in *pep4Δvps23Δ* cells. FM4-64 labeling and nitrogen starvation were performed as described in Fig. 2C. Arrows indicate accumulated GFP-Ypk1 at the perivacuolar structures where FM4-64 was strongly incorporated. Percentages noted below the images represent frequencies of the indicated phenotypes. Bar, 5 μm.

**FIGURE S5. GFP-Ypk1 is sorted into vacuoles in nitrogen-starved *pep4Δend3Δ* cells.**

Fluorescence microscopic analyses of GFP-Ypk1 localization in PMSF-treated *pep4Δend3Δ* cells. Nitrogen starvation was performed as described in Fig. 2C. Arrows indicate accumulated GFP-Ypk1 in intravacuolar space. Percentages noted below the images represent frequencies of the indicated phenotypes. Bar, 5 μm.

**FIGURE S6. Localization of Tat2-EGFP in *pep4Δend3Δ* and *pep4Δvps23Δ* cells**

(A) Fluorescence microscopic analyses of Tat2-EGFP localization in *pep4Δend3Δ* cells. Nitrogen starvation was performed as described in Fig. 2C. (B-C) Fluorescence microscopic analyses of Tat2-EGFP localization in *pep4Δvps23Δ* cells. FM4-64 labeling and nitrogen starvation were performed as described in Fig. 2C. Arrows indicate perivacuolar Tat2-EGFP localization, and arrowheads point to FM4-64-incorporated structures. Fluorescence intensity collected along a line was normalized to the maximum intensity in each channel. Relative fluorescence intensities of Tat2-EGFP (*green*) and FM4-64 (*red*) are plotted (C). Percentages noted with images represent frequencies of the indicated phenotypes. Bar, 5 μm.

**FIGURE S7. FM4-64-incorporated structures do not co-localize with Tat2-EGFP inside vacuoles of *pep4Δ* cells.**

(A-B) Fluorescence microscopic analyses of Tat2-EGFP localization in *pep4Δ* cells. FM4-64 labeling and nitrogen starvation were performed as described in Fig. 2C. Arrows indicate intravacuolar Tat2-EGFP localization, and arrowheads point to FM4-64-incorporated structures. Fluorescence intensity collected along a line was

normalized to the maximum intensity in each channel. Relative fluorescence intensities of Tat2-EGFP (*green*) and FM4-64 (*red*) are plotted (*B*). Percentages noted below the images represent frequencies of the indicated phenotypes. Bar, 5  $\mu$ m.

**FIGURE S8. GFP-Ypk1 closely associates with RFP-Atg8 within vacuoles of nitrogen-starved *pep4* $\Delta$  cells.**

Confocal microscopic analyses of GFP-Ypk1 localization with over-expressed RFP-Atg8 in PMSF-treated *pep4* $\Delta$  cells harboring pRS413-*GFP-YPK1* and Yep351-*RFP-ATG8*. Nitrogen starvation and confocal microscopic analyses were performed as described in Fig. 2E. Bar, 5  $\mu$ m.

## SUPPLEMENTAL REFERENCES

- S1. Horst, M., Knecht, E. C., and Schu, P. V. (1999) *Mol Biol Cell* **10**, 2879-2889
- S2. Silles, E., Mazon, M. J., Gevaert, K., Goethals, M., Vandekerckhove, J., Leber, R., and Sandoval, I. V. (2000) *J Biol Chem* **275**, 34054-34059
- S3. Satyanarayana, C., Schroder-Kohne, S., Craig, E. A., Schu, P. V., and Horst, M. (2000) *FEBS Lett* **470**, 232-238

Table S2. Summary of screening for cells deficient in nitrogen starvation-triggered Ypk1 proteolysis

Pathway	Yeast strain	Inhibition of Ypk1 proteolysis	Genotype
Vps pathway	<i>vps27Δ</i>	+ <sup>a</sup>	Confirmed <sup>c</sup>
	<i>vps23Δ</i>	+	Confirmed
	<i>vps22Δ</i>	- <sup>b</sup>	-
	<i>vps36Δ</i>	-	-
	<i>vps2Δ</i>	-	-
Ribophagy	<i>ubp3Δ</i>	-	-
	<i>bre5Δ</i>	-	-
Endocytosis	<i>end3Δ</i>	+	Confirmed
	<i>rvs161Δ</i>	+	Confirmed
	<i>rvs167Δ</i>	+	-
	<i>sla1Δ</i>	-	-

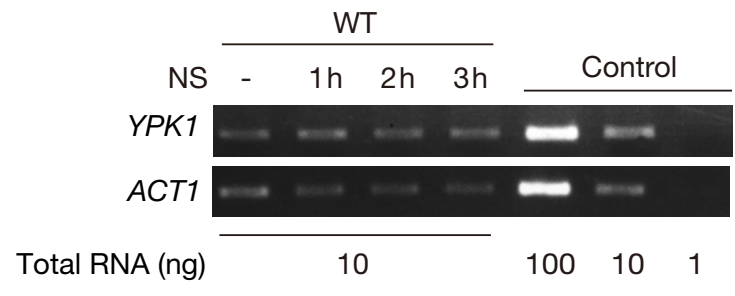
<sup>a</sup> Nitrogen starvation-induced Ypk1 proteolysis was inhibited in the strain.

<sup>b</sup> Nitrogen starvation-induced Ypk1 proteolysis was the same as in the WT strain.

<sup>c</sup> Deletion of the gene was confirmed by PCR.



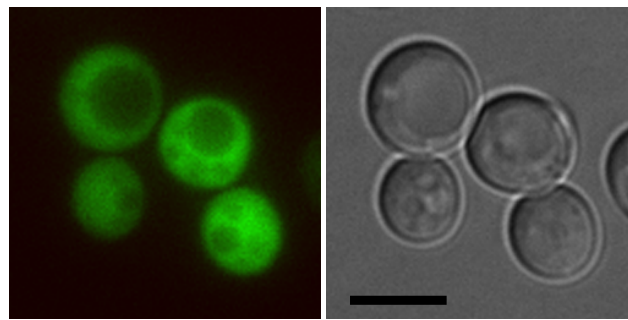
FIGURE S1



WT (pRS415-*GFP-YPK1*)

GFP-Ypk1

DIC



98.3%, n=116

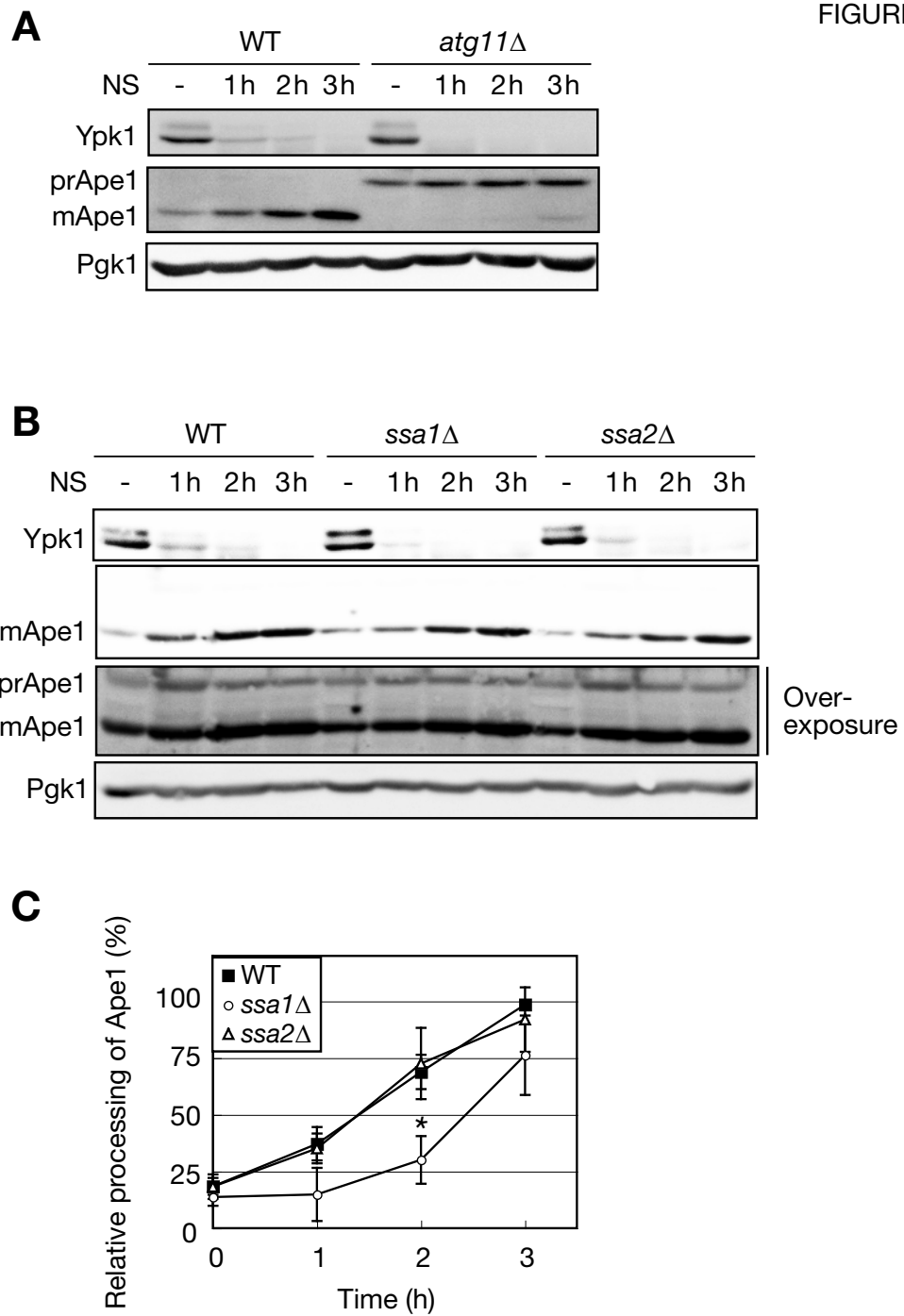


FIGURE S4

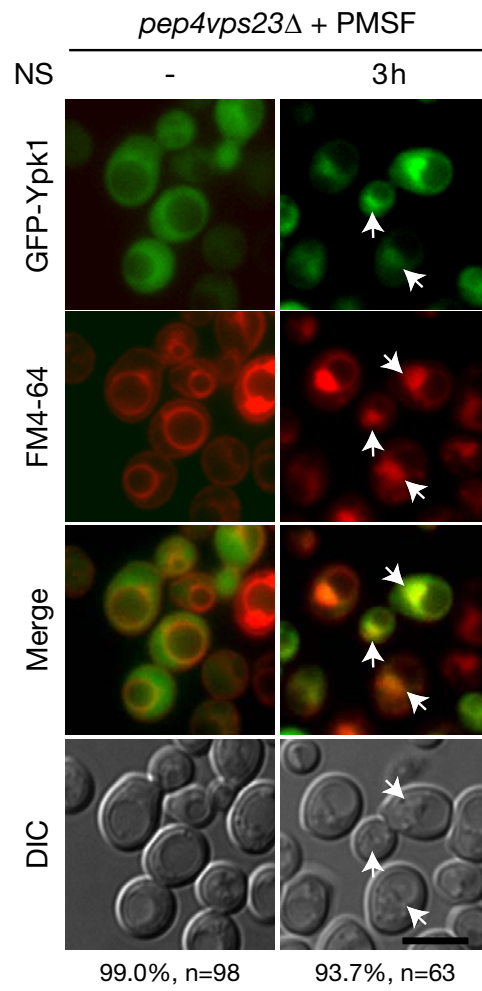
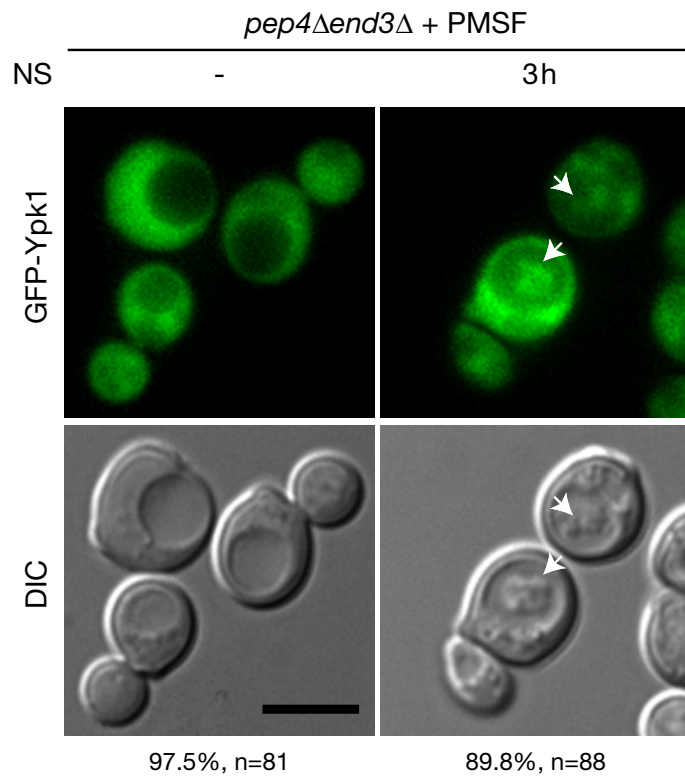
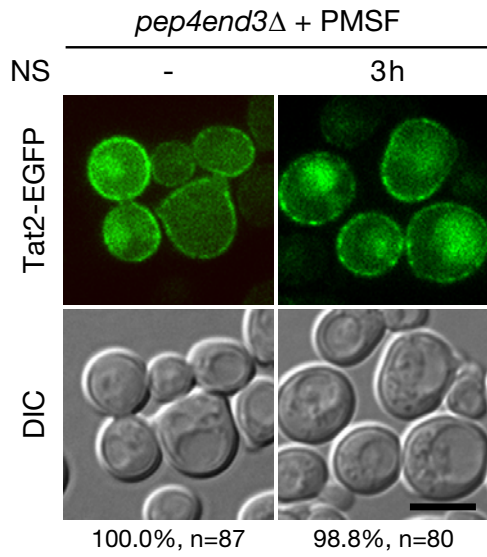


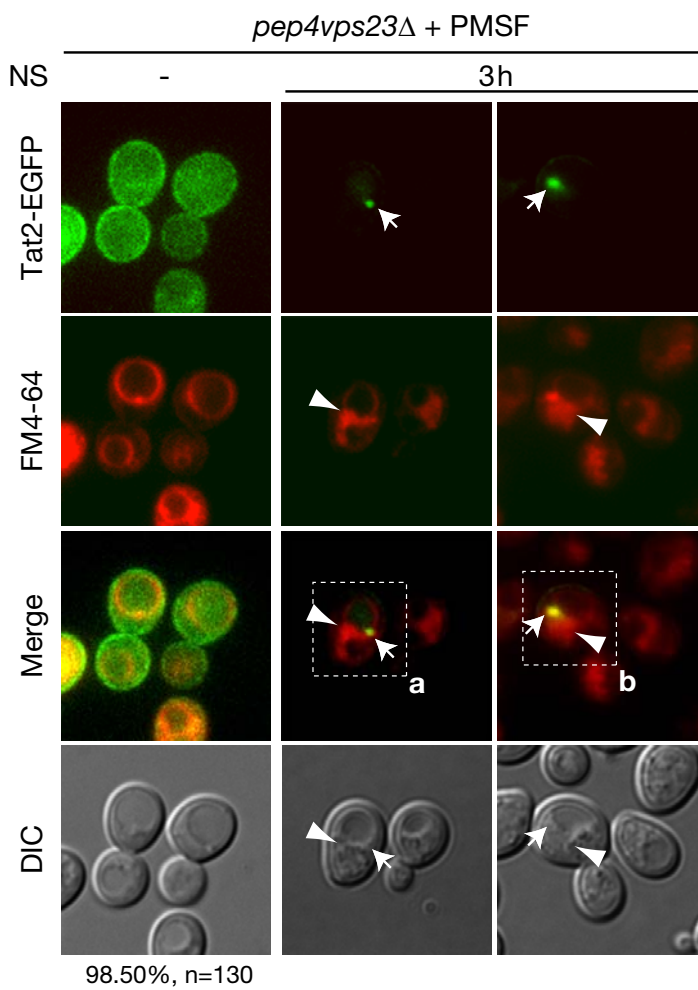
FIGURE S5



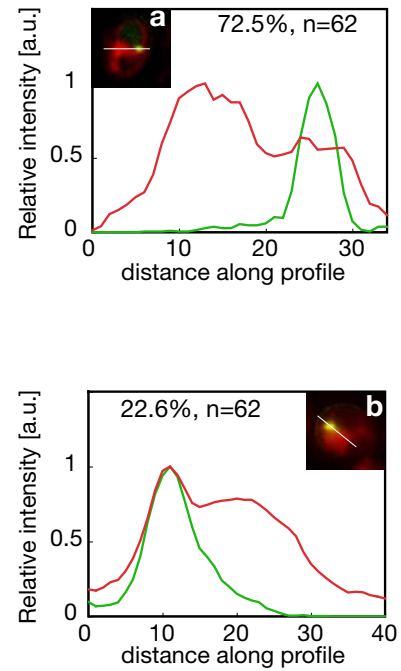
**A**



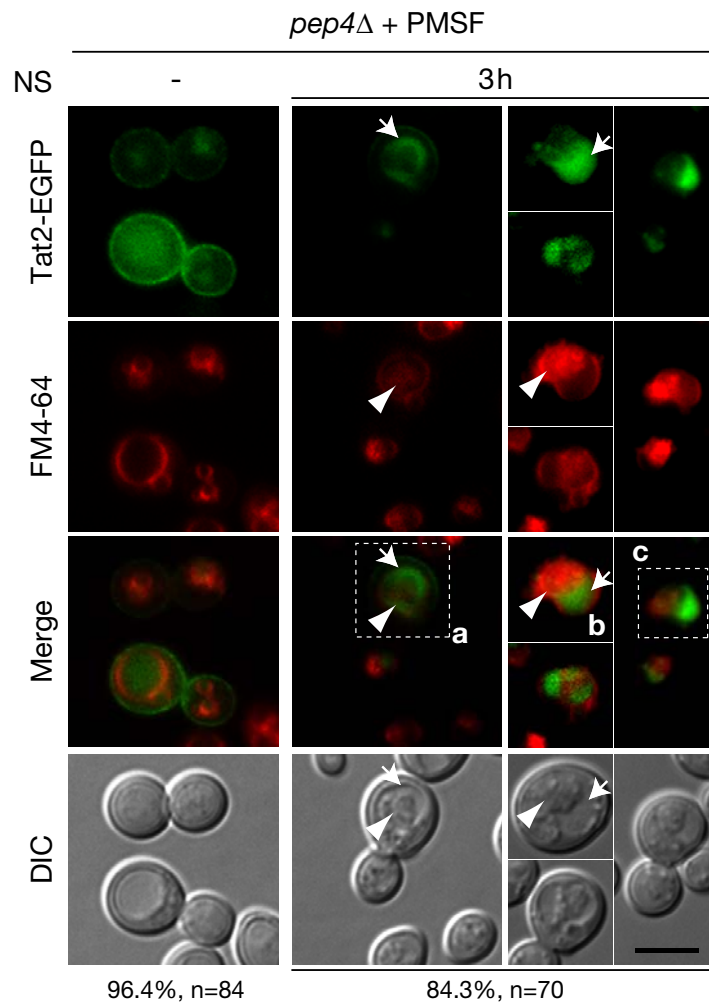
**B**



**C**



**A**



**B**

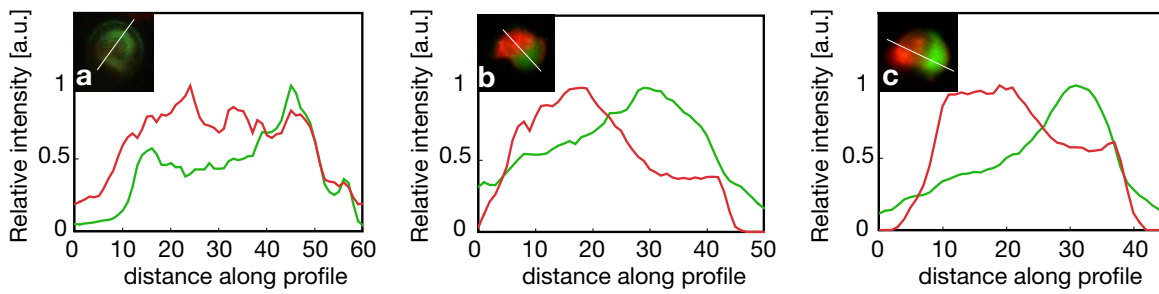


FIGURE S8

*pep4* $\Delta$  (pRS413-GFP-YPK1 and YEp351-RFP-ATG8)  
Nitrogen starvation (3h) + PMSF

